

Cite this: *RSC Adv.*, 2017, 7, 23114

# Facile preparation of hybrid vesicles loaded with silica nanoparticles *via* aqueous photoinitiated polymerization-induced self-assembly†

Jianbo Tan,<sup>a</sup> Dongdong Liu,<sup>a</sup> Xuechao Zhang,<sup>a</sup> Chundong Huang,<sup>a</sup> Jun He,<sup>a</sup> Qin Xu,<sup>a</sup> Xueliang Li<sup>a</sup> and Li Zhang<sup>\*ab</sup>

We report a room-temperature photoinitiated polymerization-induced self-assembly (photo-PISA) of 2-hydroxypropyl methacrylate (HPMA) in the presence of silica nanoparticles using a poly(ethylene glycol) methyl ether (mPEG) macromolecular chain transfer agent (macro-CTA). Hybrid vesicles loaded with silica nanoparticles were obtained by this one-pot approach. The solids content of the polymer vesicles can be up to 25% w/w. A control experiment was conducted to prove that free silica nanoparticles can be removed *via* centrifugation-redispersion. Finally, CO<sub>2</sub>-responsive hybrid vesicles were prepared by photo-PISA of HPMA and 2-(dimethylamino)ethyl methacrylate (DMAEMA). Silica nanoparticles were subsequently released from the vesicles *via* CO<sub>2</sub> bubbling at room temperature.

Received 7th March 2017

Accepted 17th April 2017

DOI: 10.1039/c7ra02770b

rsc.li/rsc-advances

## Introduction

Inorganic/organic hybrid vesicles with nanoparticles have attracted continuing interest due to their broad applications in UV screening, catalysis, cell targeting, imaging, and drug delivery.<sup>1–4</sup> One significant advantage of inorganic/organic hybrid vesicles is that they synergetically combine the inherent properties of both inorganic nanoparticles and organic vesicles.

The preparation of inorganic/organic hybrid vesicles is usually achieved by a two-step procedure using polymer vesicles as the template. In a typical procedure, polymer vesicles are firstly prepared by solution self-assembly of block copolymers and subsequently loaded with nanoparticles *via in situ* deposition. For example, Du *et al.*<sup>1</sup> reported the synthesis of hybrid polymer/titanium dioxide vesicles *via* selective deposition of tetrabutyl titanate in the PDMAEMA shell. The obtained hybrid vesicles exhibit excellent UV-screening efficacy due to the scattering by vesicles. Ren *et al.*<sup>5</sup> synthesized vesicles based on the self-assembly of poly(ethylene oxide)-*block*-poly(*tert*-butyl acrylate-*stat*-acrylic acid). Superparamagnetic iron oxide nanoparticles were then loaded *in situ* within the membrane of the vesicles. The obtained hybrid vesicles can be further used for MRI imaging and drug delivery. As an alternative, inorganic/

organic hybrid vesicles can also be prepared by self-assembly of block copolymers and nanoparticles with nanoparticles embedded into the vesicular membrane. Duan *et al.*<sup>3</sup> reported the preparation of plasmonic vesicular structures assembled from gold nanoparticles with mixed polymer brush coatings. The disruption of vesicles can be triggered by NIR irradiation, which shows potential applications in drug delivery. Liu *et al.*<sup>6</sup> developed a strategy to prepare hybrid vesicles with well-defined morphology, shape, and surface pattern by coassembling of block copolymer-coated inorganic nanoparticles and block copolymers. Bian *et al.*<sup>7</sup> reported a general UV-triggered method for assembling thiol-capped inorganic nanoparticles (including Au, Pt, Pd, and CdSe) into vesicles. The driving force of the formation of vesicles is based on oxidation of thiol ligands upon UV irradiation.

Despite the tremendous progress made in hybrid vesicles, however, these techniques are typically only conducted in dilution solution (<1%). Moreover, post-polymerization processing (*e.g.* dialysis, pH switch) is usually required to obtain diblock copolymer vesicles, which is difficult to implement on a large scale. In contrast, the recent development of polymerization-induced self-assembly (PISA) *via* reversible addition-fragmentation chain transfer (RAFT)-mediated dispersion polymerization enables diblock copolymer vesicles to be prepared at up to 30% solids content without any post-polymerization processing.<sup>8–16</sup> Recently, the preparation of hybrid vesicles *via* PISA has been explored by several groups. For example, the Boyer group<sup>2</sup> synthesized diblock copolymer vesicles *via* alcoholic dispersion polymerization of styrene at 70 °C. Gold nanoparticles were then attached to the vesicles *via* post reduction. Zhou *et al.*<sup>17</sup> reported the synthesis of poly(2-(acetoxetoxy)ethyl methacrylate)-based vesicles *via* alcoholic

<sup>a</sup>Department of Polymeric Materials and Engineering, School of Materials and Energy, Guangdong University of Technology, Guangzhou 510006, China. E-mail: tanjianbo@gdut.edu.cn; lizhang@gdut.edu.cn

<sup>b</sup>Guangdong Provincial Key Laboratory of Functional Soft Condensed Matter, Guangzhou 510006, China

† Electronic supplementary information (ESI) available. See DOI: 10.1039/c7ra02770b

dispersion polymerization, and silver nanoparticles were formed after complexation of  $\text{Ag}^+$  with the ketoester group. Mable *et al.*<sup>18</sup> reported the synthesis of silica-loaded polymer vesicles *via* aqueous dispersion polymerization in the presence of silica nanoparticles at 70 °C. Silica nanoparticles can be released from the vesicles by decreasing the temperature to 0 °C. Very recently, Zheng *et al.*<sup>19</sup> developed a surface-initiated alcoholic PISA formulation of polymer-grafted silica nanoparticles to prepare single-walled hybrid vesicles at 70 °C. However, precipitation occurred at high monomer conversions which may be ascribed to irregular particle aggregation.

Herein, we report a room-temperature strategy to prepare hybrid polymer vesicles *via* aqueous photoinitiated RAFT dispersion polymerization of HPMA. The solids content can be up to 25% w/w. Water-dispersible silica nanoparticles (20 nm) were added at the beginning of the reaction and encapsulated *in situ* into the polymer vesicles. Finally, silica nanoparticles were released from  $\text{CO}_2$ -responsive polymer vesicles *via*  $\text{CO}_2$  trigger under mild conditions.

## Experimental section

### Materials

2-Hydroxypropyl methacrylate (HPMA, Aladdin), poly(ethylene glycol) methyl ether (Sigma Aldrich, mPEG<sub>113</sub>,  $M_n = 5000 \text{ g mol}^{-1}$ ), poly(ethylene glycol) methyl ether methacrylate (PEGMA,  $M_n = 500 \text{ g mol}^{-1}$ ), 2-(dimethylamino)ethyl methacrylate (DMAEMA, Aladdin), 1,3,5-trioxacyclohexane (Aladdin), dicyclohexylcarbodiimide (DCC, Aladdin), 4-dimethylaminopyridine (DMAP, Aladdin), hydroquinone (Aladdin), 2,4,6-trimethylbenzoyldi-phenylphosphine (TPO-L, Tianjin Jiuri Chemical Co., LTD), and LUDOX® AM colloidal silica (30 wt% suspension in  $\text{H}_2\text{O}$ , Sigma-Aldrich) were used without further purification. 2,2-Azobisisobutyronitrile (AIBN, Aladdin) was recrystallized from ethanol prior to storage under refrigeration at 4 °C. Sodium phenyl-2,4,6-trimethylbenzoylphosphine (SPTP) was synthesized according to a literature procedure.<sup>20</sup> 4-Cyano-4-(ethylthiocarbonothioylthio) pentanoic acid (CEPA) and 4-cyano-4-(dodecylsulfanylthiocarbonyl) sulfanylpentanoic acid (CDPA) were synthesized according to literature.<sup>21</sup>

### Synthesis of mPEG<sub>113</sub>-CEPA

A solution of CEPA (1.20 g, 4.40 mmol) in anhydrous dichloromethane (40 mL) was introduced in a dry flask under nitrogen atmosphere containing mPEG<sub>113</sub> (11.00 g, 2.20 mmol). Then a solution of DCC (0.90 g, 4.40 mmol) and DMAP (0.054 g, 0.44 mmol) in anhydrous dichloromethane (10 mL) was added dropwise to the reaction mixture at 0 °C. The esterification reaction proceeded with stirring at room temperature for 48 h. The product was collected by precipitation in cold diethyl ether, and washed several times with additional diethyl ether. The product was finally dried at 45 °C under vacuum to obtain a yellow powder.

### Synthesis of PPEGMA<sub>14</sub>-CDPA

PEGMA (7.50 g, 15.00 mmol), CDPA (0.40 g, 1.00 mmol), AIBN (0.033 g, 0.20 mmol), and 1,3,5-trioxacyclohexane (0.14 g, 1.50 mmol), and 1,4-dioxane (10.0 g) were added into a 50 mL round bottom flask. The reaction mixture was purged with nitrogen, sealed, and immersed into a preheated oil bath at 70 °C for 5 h (monomer conversion = 90% as determined by  $^1\text{H}$  NMR). The reaction was quenched by immersion in ice/water and exposure to air. The macro-RAFT agent was precipitated with cold diethyl ether and washed several times with additional diethyl ether. The product was dried at 45 °C under vacuum overnight.

### Aqueous photoinitiated RAFT dispersion polymerization

A typical protocol for the synthesis of mPEG<sub>113</sub>-PHPMA<sub>365</sub> vesicles is given below: HPMA (2.50 g, 0.017 mol), mPEG<sub>113</sub>-CEPA (0.25 g, 0.048 mmol), SPTP (5.0 mg, 0.016 mmol), and water (7.50 g) were added into a 25 mL round bottom flask. The reaction mixture was purged with nitrogen for 20 min, sealed, and irradiated by a LED lamp (405 nm, light intensity of  $0.4 \text{ mW cm}^{-2}$ ) at room temperature for 1 h.

### *In situ* encapsulation of silica nanoparticles into vesicles

A typical protocol for the synthesis of hybrid vesicles is given below: HPMA (2.50 g, 0.017 mol), mPEG<sub>113</sub>-CEPA (0.25 g, 0.048 mmol), SPTP (5.0 mg, 0.016 mmol), silica sol (4.0 g, 30%) and water (4.70 g) were added into a 25 mL round bottom flask. The reaction mixture was purged with nitrogen for 20 min, sealed, and irradiated by a LED lamp (405 nm, light intensity of  $0.4 \text{ mW cm}^{-2}$ ) for 1 h. The obtained vesicles were diluted with water, sedimented by centrifugation at 4000 rpm and resuspended in water. This washing process was repeated 8 times to remove free silica nanoparticles. It should be noted that the concentration of HPMA in water was maintained at 25% w/w for all formulations.

### Synthesis of $\text{CO}_2$ -responsive hybrid vesicles

For the synthesis of mPEG<sub>113</sub>-P(HPMA<sub>365</sub>-*co*-DMAEMA<sub>40</sub>) hybrid vesicles, HPMA (1.0 g, 6.9 mmol), mPEG<sub>113</sub>-CEPA (0.10 g, 0.019 mmol), SPTP (2.10 mg, 0.016 mmol), DMAEMA (0.13 g, 0.80 mmol), silica sol (1.60 g, 30%), and water (1.90 g) were added into a 25 mL round bottom flask. The reaction mixture was purged with nitrogen for 20 min, sealed, and irradiated by a LED lamp (405 nm, light intensity of  $0.4 \text{ mW cm}^{-2}$ ) for 1 h. The obtained vesicles were diluted with water, sedimented by centrifugation at 4000 rpm and resuspended in water. This washing process was repeated 8 times to remove free silica nanoparticles.

### Characterization

The products were diluted 100-fold with water. A drop of the dispersion was placed on a copper grid for 1 min and then blotted with filter paper to remove excess solution. Then a drop of uranyl acetate solution (0.5% w/w) was soaked on the same copper grid for 1.5 min, and then blotted using filter paper to remove excess solution. Transmission electron microscopy



(TEM) observations were carried out on a FEI Tecnai G2 Spirit instrument operated at 120 kV or a ZEISS GeminiSEM500 instrument operated at 22 kV. Scanning electron microscopy (SEM) observations were carried out on a ZEISS GeminiSEM500 instrument operated at 2 kV or lower.

Copolymer molecular weights and polydispersities were determined by gel permeation chromatography (GPC) instrument using a Waters 1515 instrument with tetrahydrofuran (THF) as the mobile phase and Waters Styragel HR1, HR4 columns. The flow rate of THF was 1.0 mL min<sup>-1</sup>. Calibration was conducted using near-monodisperse poly(methyl methacrylate) standards.

<sup>1</sup>H NMR measurements were conducted in D<sub>2</sub>O or DMSO-*d*<sub>6</sub> using a Bruker Advance III NMR spectrometer (400 MHz) at 25 °C.

Hydrodynamic diameters of the dispersions (0.1% v/v) were conducted using Brookhaven nanoparticle size-zeta potential *t* analyzers.

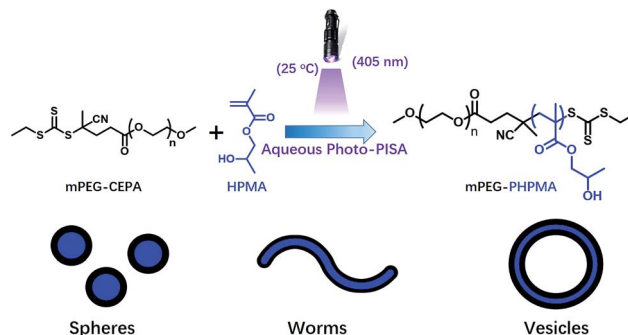
Thermogravimetric analysis (TGA) was performed using a SDT 2960 Simultaneous DSC-TGA instrument under a stream of nitrogen. The samples were heated from 50 to 700 °C at a scan rate of 10 °C min<sup>-1</sup>.

## Results and discussion

### Photoinitiated polymerization-induced self-assembly

Polymerization-induced self-assembly is typically conducted *via* thermal initiation at 70 °C, which may limit the preparation of thermo-sensitive or bio-related polymer nano-objects. Recently, our group developed an aqueous photoinitiated polymerization-induced self-assembly (photo-PISA) of HPMA at low temperatures, and quantitative monomer conversions were achieved in a short reaction time (<15 min).<sup>22–25</sup> Globular proteins and silica nanoparticles can be encapsulated *in situ* into vesicles *via* photo-PISA. In the present work, we further investigate the photo-PISA strategy for the preparation of hybrid vesicles by adding silica nanoparticles at the beginning of the reaction. This strategy provides a prototype to prepare vesicles with different payloads. In particular, the low temperature property of this method is beneficial for encapsulating thermo-sensitive payloads into the vesicles.

The macro-RAFT agent (mPEG<sub>113</sub>-CEPA) was synthesized by esterification of mPEG<sub>113</sub> and CEPA in anhydrous dichloromethane for 48 h at room temperature. mPEG<sub>113</sub>-CEPA was subsequently chain extended to synthesize well-defined diblock copolymer nano-objects *via* aqueous photo-PISA of HPMA at 25 °C under 405 nm visible light irradiation, as shown in Scheme 1. A kinetic study of aqueous photo-PISA of HPMA (target degree of polymerization (DP) of 200) was conducted at room temperature with a HPMA concentration of 10% w/w (Fig. S1†). The polymerization proceeded rapidly with 100% monomer conversion (determined by <sup>1</sup>H NMR of the disappearance of vinyl signals) being reached within 15 min of 405 nm visible light irradiation. This can be attributed to the fast decomposition of photoinitiator (SPTP in the present work) under 405 nm visible light irradiation.



**Scheme 1** Synthesis of poly(ethylene glycol)-*b*-poly(2-hydroxypropyl methacrylate) diblock copolymer nano-objects *via* aqueous photo-initiated polymerization-induced self-assembly at 25 °C.

One advantage of PISA is that the morphology of polymer nano-objects (spheres, worms, and vesicles) can be controlled by varying the DP of the core-forming block and monomer concentration. Fig. 1 shows TEM images of mPEG<sub>113</sub>-PHPMA<sub>*n*</sub> (*n* = 100, 200, 365) diblock copolymer nano-objects prepared at different monomer concentrations (10%, 20%, and 25%). Pure spheres, worms, and vesicles were obtained by aqueous photo-PISA. Fig. 1d shows GPC results for the corresponding mPEG<sub>113</sub>-PHPMA<sub>*n*</sub> (*n* = 100, 200, 365) diblock copolymers and mPEG<sub>113</sub>-CEPA. It can be clearly seen that increasing the target DP of PHPMA block leads to a monotonic increase in the GPC molecular weight of the diblock copolymers. Narrow molecular weight distributions ( $M_w/M_n < 1.30$ ) were observed in all studied

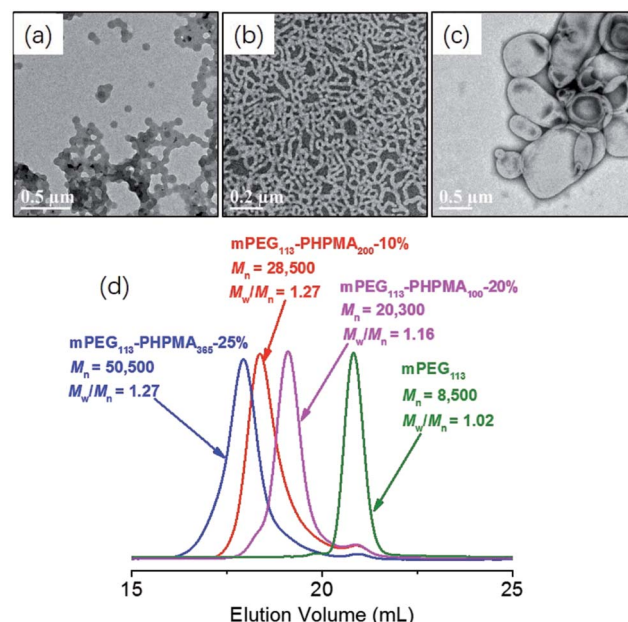


**Fig. 1** TEM images of mPEG<sub>113</sub>-PHPMA<sub>*n*</sub> diblock copolymer nano-objects prepared *via* aqueous photo-PISA at different HPMA concentrations: (a) *n* = 200, 10% w/w HPMA, (b) *n* = 100, 20% w/w HPMA, (c) *n* = 365, 25% w/w; (d) GPC traces of mPEG<sub>113</sub> and mPEG<sub>113</sub>-PHPMA<sub>*n*</sub> (*n* = 100, 200, 365) diblock copolymers prepared *via* aqueous photo-PISA at different HPMA concentrations.





formulations. These results indicated that good control was maintained during the aqueous photo-PISA process. It should be noted that the obtained diblock copolymers contained modest levels of low molecular weight impurities according to the GPC results. This can be attributed to the presence of a small amount of non-functionalized mPEG<sub>113</sub>.

### Synthesis and characterization of hybrid vesicles loaded with silica nanoparticles

It is well-known that polymer vesicles are hollow spheres with a hydrophobic membrane and hydrophilic interior that can encapsulate both hydrophobic and hydrophilic payloads.<sup>26</sup> We then attempted to load silica nanoparticles into polymer vesicles *via* aqueous photo-PISA. Commercial available silica sol (containing 30% w/w silica nanoparticles in water, 20 nm) was added at the beginning of aqueous photo-PISA and became encapsulated *in situ* in the lumen of polymer vesicles as shown in Scheme 2. Free silica nanoparticles can be removed *via* a careful centrifugation-redispersion process. It should be noted that the concentration of HPMA was maintained at 25% w/w in all formulations with the consideration of additional water content in the silica sol.

Milky white and highly viscous dispersions were obtained by varying amounts of silica nanoparticle sol from 0 to 6.0 g. <sup>1</sup>H NMR measurement confirmed that high monomer conversions (>98%) were achieved in all cases, suggesting that the presence of silica nanoparticles did not disturb the aqueous photo-PISA process. Fig. 2 shows TEM images of the silica/mPEG<sub>113</sub>-PHPMA<sub>365</sub> hybrid vesicles prepared *via* aqueous photo-PISA of HPMA at room temperature before and after centrifugation. It can be clearly seen that silica-loaded hybrid vesicles were contaminated with free silica nanoparticles before the centrifugation-redispersion process (Fig. 2a, d and g), and a large number of free silica nanoparticles were present when the adding amount of silica sol was 6.0 g (see Fig. 2g). After nine centrifugation-redispersion cycles (centrifuged at 4000 rpm), TEM images confirmed that most free silica nanoparticles had been removed and hybrid vesicles were obtained. Comparing Fig. 2c and f, it is clear that more silica nanoparticles were encapsulated into the vesicles as the adding amount of silica sol increased from 2.0 to 4.0 g.

One may question these TEM observations are the result of drying artifacts. We then conducted a control experiment to ensure that silica nanoparticles are indeed encapsulated inside the vesicles. Pure mPEG<sub>113</sub>-PHPMA<sub>365</sub> vesicles were mixed with a certain amount of silica nanoparticles (comparable with the sample of Fig. 2d) under magnetic stirring for 1 h. Fig. 3a shows

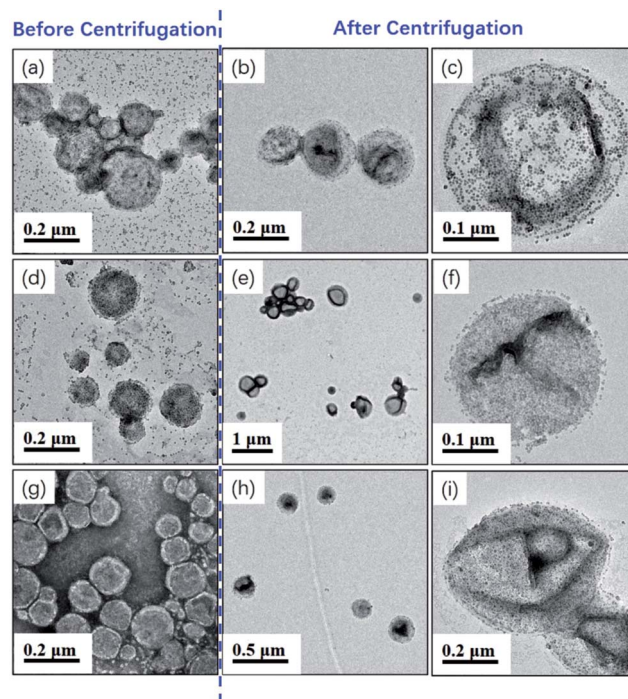
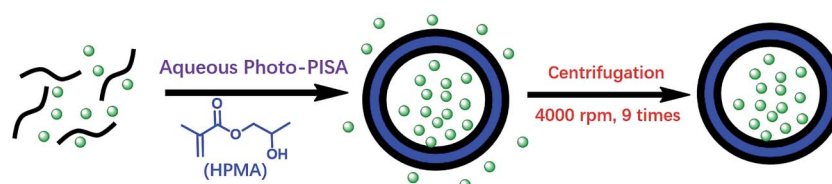


Fig. 2 TEM images of unpurified and purified mPEG<sub>113</sub>-PHPMA<sub>365</sub> hybrid vesicles prepared *via* aqueous photo-PISA of HPMA by adding different amounts of silica sol (30% in water): (a)–(c) 2.0 g; (d)–(f) 4.0 g; (g)–(i) 6.0 g.

the TEM image of the sample and vesicles contaminated with a large number of free silica nanoparticles are observed. The sample was then subjected to nine centrifugation-redispersion cycles (centrifuged at 4000 rpm) to remove free silica nanoparticles. Fig. 3b shows that majority of silica nanoparticles have been removed and only a few silica nanoparticles contaminated with the vesicles (Fig. 3b). TGA measurement further confirmed this conclusion (Fig. 3c). The hybrid vesicles prepared with 4.0 g silica sol (Fig. 2d) were then characterized by SEM as shown in Fig. 4a. It should be noted that the operating voltage should be lower than 2.0 kV to maintain the morphology of hybrid vesicles under high vacuum conditions. Fig. 4a shows the SEM image of the sample before centrifugation. A large number of silica nanoparticles were observed on the surface of the vesicle. After nine centrifugation-redispersion cycles, only a few silica nanoparticles were attached on the surface of the vesicle (Fig. 4b), indicating that vast majority of free silica nanoparticles have been removed. The same vesicle of Fig. 4b was then characterized under STEM mode and the STEM



Scheme 2 Preparation and purification of hybrid vesicles loaded with silica nanoparticles *via* aqueous photo-PISA of HPMA.



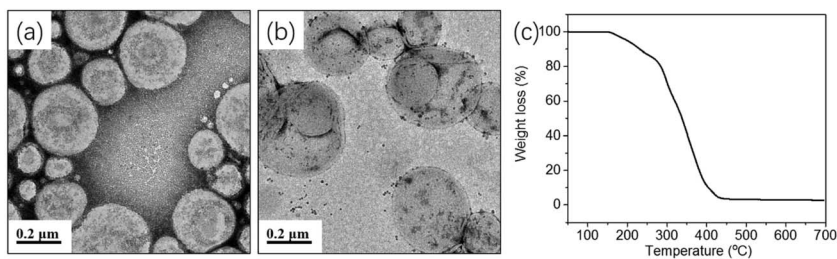


Fig. 3 (a) TEM image of the mPEG<sub>113</sub>-PPHMA<sub>365</sub> vesicles mixed with silica nanoparticles under magnetic stirring for 1 h, (b) the sample of (a) after nine centrifugation-redispersion cycles, (c) TGA curve of sample (b).

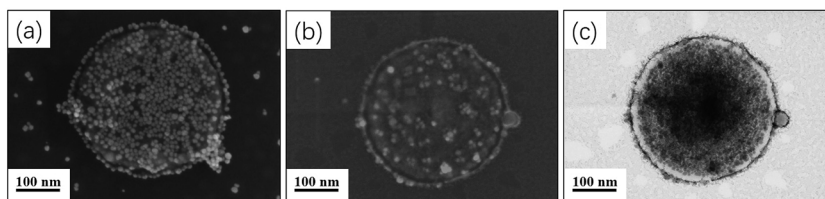


Fig. 4 (a) SEM image of unpurified mPEG<sub>113</sub>-PPHMA<sub>365</sub> hybrid vesicles prepared *via* aqueous photo-PISA of HPMA in the presence of 4.0 g silica sol, (b) SEM image of purified mPEG<sub>113</sub>-PPHMA<sub>365</sub> hybrid vesicles prepared *via* aqueous photo-PISA of HPMA in the presence of 4.0 g silica sol, (c) STEM image of the same vesicle of (b).

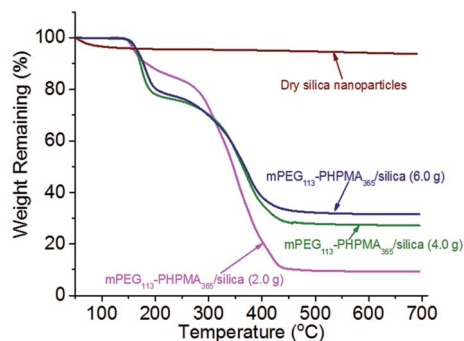


Fig. 5 TGA data recorded for purified mPEG<sub>113</sub>-PPHMA<sub>365</sub> diblock copolymer vesicles prepared in the presence of increasing amounts of silica sol. TGA curve for the dried silica nanoparticles was also measured as a reference.

image indicated that a large number of silica nanoparticles were still encapsulated inside the vesicular lumen (Fig. 4c). TGA was then utilized to characterize the purified hybrid vesicles as shown in Fig. 5. The weight loss below 450 °C can be assigned to the loss of PPHMA vesicles. No weight loss was observed at above 450 °C, indicating the remaining of silica nanoparticles. Higher percentage of weight remaining was observed as the increase of adding amount of silica nanoparticles, indicating more silica nanoparticles were encapsulated into the lumen of vesicles.

A linear polymer was used as the macro-RAFT agent (mPEG<sub>113</sub>-CEPA) in the above aqueous photo-PISA for the preparation of hybrid vesicles. In order to gain further insight into the formation process of hybrid vesicles, PPEGMA<sub>14</sub>-CDPA, a brush-type macro-RAFT was then utilized to mediate the

aqueous photo-PISA process. According to our previous work,<sup>24</sup> pure vesicles can be obtained by aqueous photo-PISA of HPMA at a monomer concentration of 20% w/w with the target DP of 400. Similar results were observed in the present work, as shown in Fig. 6a and b. We then attempted to encapsulate silica nanoparticles into these vesicles *via* aqueous photo-PISA using

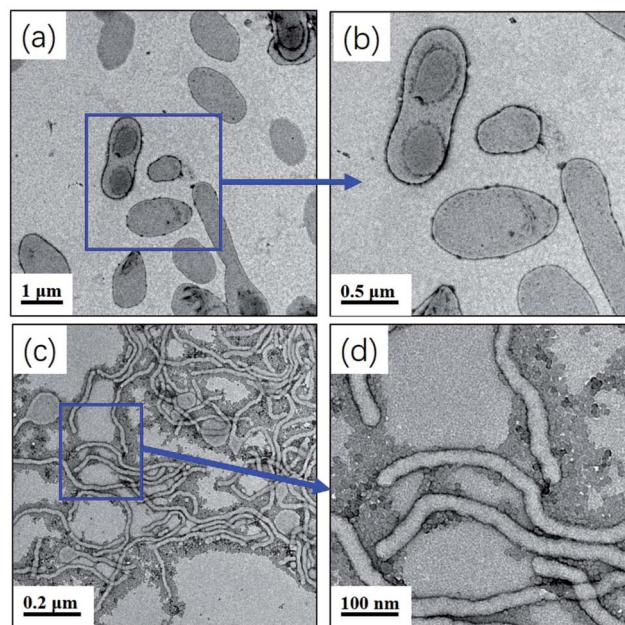
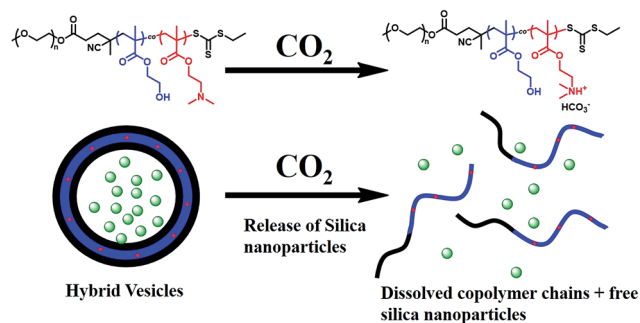


Fig. 6 (a) and (b) TEM images of PPEGMA<sub>14</sub>-PPHMA<sub>400</sub> diblock copolymer vesicles *via* aqueous photo-PISA (20% w/w HPMA); (c) and (d) TEM images of PPEGMA<sub>14</sub>-PPHMA<sub>400</sub> diblock copolymer nano-objects *via* aqueous photo-PISA with 4.0 g silica sol added at the beginning of the reaction.







Scheme 3  $\text{CO}_2$ -triggered release of silica nanoparticles from  $\text{mPEG}_{113}\text{-P}(\text{HPMA}_{365}\text{-co-DMAEMA}_{40})$  hybrid vesicles.

the brush-type macro-RAFT agent. 4.0 g silica sol was added to the above formulation and the concentration of HPMA was maintained at 20% w/w with the consideration of water content in the silica sol. High monomer conversion (>99%) was observed in this case, however, no hybrid vesicles were observed. Fig. 6c shows the TEM image of the obtained sample and only worm-like micelles were formed. The high magnification TEM image (Fig. 6d) shows that a large number of silica nanoparticles were contaminated with the worm-like micelles. These results indicate that the presence of silica nanoparticles limited the formation of higher order morphologies (vesicles in this case) when a brush-type macro-RAFT agent was used in

aqueous photo-PISA. Qiao *et al.*<sup>27</sup> reported that the adsorbed amount of PPEGMA on silica surface at saturation ( $1.87 \text{ mg m}^{-2}$ ) is significant higher than that of the linear PEO (around  $0.4\text{--}0.8 \text{ mg m}^{-2}$ ). Therefore, the adsorption of PPEGMA-CDPA on silica nanoparticles increases the effective volume fraction of the PPEGMA stabilizer block and hence lowers the packing parameter, which restricts the formation of vesicles. In contrast, the adsorption of mPEG-CEPA on the silica nanoparticles is relatively low, which has little effect on the parameter of the copolymer chains. Thus it is important to weaken the interaction between the macro-RAFT agent and nanoparticles when preparing hybrid vesicles *via* aqueous photo-PISA.

### $\text{CO}_2$ -triggered release of silica nanoparticles

Release of inorganic nanoparticles from vesicles *via* environmental stimulus has potential applications in self-healing materials, catalysis, and drug delivery.<sup>3,28,29</sup> In particular,  $\text{CO}_2$  responsiveness has attracted numerous attentions due to the mild and green property, as well as the robust switchability. Moreover,  $\text{CO}_2$  is an important metabolite for life and has good membrane permeability and biocompatibility.<sup>30–33</sup> Recently, our group developed an aqueous photo-PISA formulation for the preparation of  $\text{CO}_2$ -responsive polymer vesicles by introducing DMAEMA into the core-forming block. Bovine serum albumin (BSA) can be encapsulated and subsequently released *via*  $\text{CO}_2$ -trigger under mild conditions.<sup>23</sup>

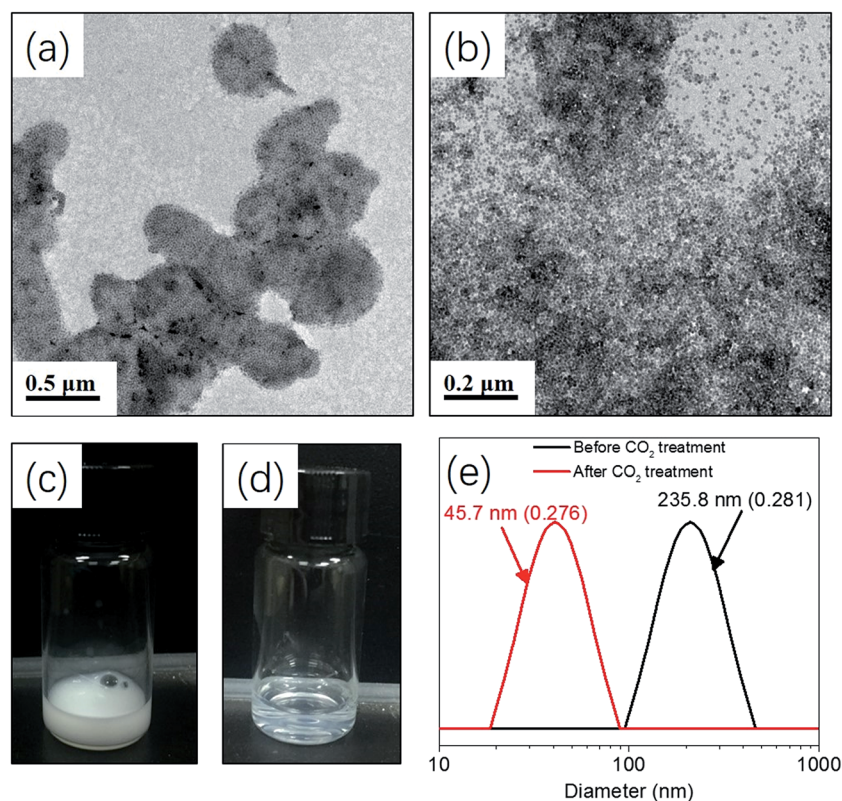


Fig. 7 (a) TEM image of  $\text{mPEG}_{113}\text{-P}(\text{HPMA}_{365}\text{-co-DMAEMA}_{40})$  hybrid vesicles prepared by aqueous photo-PISA of HPMA and DMAEMA, (b) TEM image of sample (a) after bubbling with  $\text{CO}_2$ , (c) digital photo of the dispersion of sample (a), (d) digital photo of the dispersion of sample (b), (e) DLS measurement of  $\text{mPEG}_{113}\text{-P}(\text{HPMA}_{365}\text{-co-DMAEMA}_{40})$  hybrid vesicles before and after  $\text{CO}_2$  treatment.



Herein, hybrid CO<sub>2</sub>-responsive vesicles were prepared by aqueous photo-PISA of HPMA and DMAEMA by adding 4.0 g silica sol at the beginning of the polymerization. The target composition of the copolymer was mPEG<sub>113</sub>-P(HPMA<sub>365</sub>-co-DMAEMA<sub>40</sub>) prepared with 25% w/w of HPMA. Silica nanoparticles can be released from the vesicles *via* CO<sub>2</sub> trigger as shown in Scheme 3. Fig. 7a shows that hybrid vesicles were obtained with silica nanoparticles loading inside the lumen, indicating that the presence of DMAEMA did not disturb the formation of vesicular structure. The dispersion of hybrid vesicles was then bubbling with CO<sub>2</sub> for 2 min at room temperature. It is apparent that silica nanoparticles were released from the vesicles as confirmed by TEM (Fig. 7b). This can be explained by the protonation of DMAEMA after CO<sub>2</sub> treatment, resulting in the enhanced hydrophilic of the core-forming block and thus the dissociation of hybrid vesicles. Visual appearance of the dispersions before and after CO<sub>2</sub> treatment further confirmed this conclusion. As shown in Fig. 7c and d, the original dispersion was milky white and changed to transparent after CO<sub>2</sub> treatment. DLS experiments show that the intensity-average diameter of the sample decreased from 235.8 nm (0.281) to 45.7 nm (0.276) after CO<sub>2</sub> bubbling, indicating the transformation of polymer vesicles to dissolved copolymer chains and subsequently release of silica nanoparticles. Similar results were observed by decreasing the pH from 7.0 to 5.0 (Fig. S2†). It should be noted that the hybrid vesicles could not regenerate after the removal of CO<sub>2</sub> *via* purging with nitrogen. A control experiment was also carried out by treating the silica/mPEG<sub>113</sub>-PHPMA<sub>365</sub> hybrid vesicles *via* CO<sub>2</sub> bubbling. Fig. S3† shows that the vesicular morphology was maintained after CO<sub>2</sub> treatment, confirming that DMAEMA is important for the contribution of CO<sub>2</sub> responsiveness.

## Conclusion

In summary, we report a room-temperature strategy to prepare silica/mPEG<sub>113</sub>-PHPMA<sub>365</sub> hybrid vesicles *via* aqueous photo-initiated RAFT dispersion polymerization of HPMA in the presence of different amounts of silica nanoparticles. TEM measurement confirms that hybrid vesicles are obtained with silica nanoparticle encapsulated inside the lumen of vesicles. Pure mPEG<sub>113</sub>-PHPMA<sub>365</sub> vesicles were mixed with a certain amount of silica nanoparticle and then purified by nine centrifugation-redispersion cycles. These results suggest that free silica nanoparticles can be removed *via* the centrifugation-redispersion process. PPEGMA<sub>14</sub>-CDPA, a brush-typed macro-RAFT agent was attempted to prepare hybrid vesicles, however, only worm-like micelles were obtained. Finally, CO<sub>2</sub>-responsive hybrid vesicles were prepared *via* aqueous photo-PISA of HPMA and DMAEMA in the presence of silica nanoparticles. Silica nanoparticles can be released *via* CO<sub>2</sub> trigger under mild conditions, which shows potential applications in biological areas.

## Acknowledgements

The authors acknowledge support from the National Natural Science Foundation of China (Grant 21504017), Guangdong

Natural Science Foundation (Grant 2016A030310339), and the Innovation Project of Education Department in Guangdong (Grant 2015KTSCX029). Prof. Zhaohua Zeng (Sun Yat-sen University) is thanked for the great support he provided for this work.

## References

- 1 J. Du and H. Sun, *ACS Appl. Mater. Interfaces*, 2014, **6**, 13535–13541.
- 2 R. Bleach, B. Karagoz, S. M. Prakash, T. P. Davis and C. Boyer, *ACS Macro Lett.*, 2014, **3**, 591–596.
- 3 J. Song, J. Zhou and H. Duan, *J. Am. Chem. Soc.*, 2012, **134**, 13458–13469.
- 4 Y. Liu, Y. Liu, J.-J. Yin and Z. Nie, *Macromol. Rapid Commun.*, 2015, **36**, 711–725.
- 5 T. Ren, Q. Liu, H. Lu, H. Liu, X. Zhang and J. Du, *J. Mater. Chem.*, 2012, **22**, 12329–12338.
- 6 Y. Liu, Y. Li, J. He, K. J. Dülge, Z. Lu and Z. Nie, *J. Am. Chem. Soc.*, 2014, **136**, 2602–2610.
- 7 T. Bian, L. Shang, H. Yu, M. T. Perez, L.-Z. Wu, C.-H. Tung, Z. Nie, Z. Tang and T. Zhang, *Adv. Mater.*, 2014, **26**, 5613–5618.
- 8 S. L. Canning, G. N. Smith and S. P. Armes, *Macromolecules*, 2016, **49**, 1985–2001.
- 9 N. J. Warren and S. P. Armes, *J. Am. Chem. Soc.*, 2014, **136**, 10174–10185.
- 10 J.-T. Sun, C.-Y. Hong and C.-Y. Pan, *Polym. Chem.*, 2013, **4**, 873–881.
- 11 W. Zhou, Q. Qu, Y. Xu and Z. An, *ACS Macro Lett.*, 2015, 495–499.
- 12 J. Tan, C. Huang, D. Liu, X. Zhang, Y. Bai and L. Zhang, *ACS Macro Lett.*, 2016, 894–899.
- 13 J. Yeow, J. Xu and C. Boyer, *ACS Macro Lett.*, 2015, **4**, 984–990.
- 14 Y. Pei and A. B. Lowe, *Polym. Chem.*, 2014, **5**, 2342–2351.
- 15 J. Tan, D. Liu, Y. Bai, C. Huang, X. Li, J. He, Q. Xu, X. Zhang and L. Zhang, *Polym. Chem.*, 2017, **8**, 1315–1327.
- 16 J. Tan, C. Huang, D. Liu, X. Li, J. He, Q. Xu and L. Zhang, *ACS Macro Lett.*, 2017, **6**, 298–303.
- 17 W. Zhou, Q. Qu, W. Yu and Z. An, *ACS Macro Lett.*, 2014, **3**, 1220–1224.
- 18 C. J. Mable, R. R. Gibson, S. Prevost, B. E. McKenzie, O. O. Mykhaylyk and S. P. Armes, *J. Am. Chem. Soc.*, 2015, **137**, 16098–16108.
- 19 Y. Zheng, Y. Huang, Z. M. Abbas and B. C. Benicewicz, *Polym. Chem.*, 2017, **8**, 370–374.
- 20 Y. Jiang, N. Xu, J. Han, Q. Yu, L. Guo, P. Gao, X. Lu and Y. Cai, *Polym. Chem.*, 2015, **6**, 4955–4965.
- 21 G. Moad, Y. K. Chong, A. Postma, E. Rizzardo and S. H. Thang, *Polymer*, 2005, **46**, 8458–8468.
- 22 J. Tan, Y. Bai, X. Zhang, C. Huang, D. Liu and L. Zhang, *Macromol. Rapid Commun.*, 2016, **37**, 1434–1440.
- 23 J. Tan, X. Zhang, D. Liu, Y. Bai, C. Huang, X. Li and L. Zhang, *Macromol. Rapid Commun.*, 2016, DOI: 10.1002/marc.201600508.
- 24 J. Tan, Y. Bai, X. Zhang and L. Zhang, *Polym. Chem.*, 2016, **7**, 2372–2380.



- 25 J. Tan, H. Sun, M. Yu, B. S. Sumerlin and L. Zhang, *ACS Macro Lett.*, 2015, **4**, 1249–1253.
- 26 Y. Zhu, B. Yang, S. Chen and J. Du, *Prog. Polym. Sci.*, 2017, **64**, 1–22.
- 27 X. G. Qiao, P.-Y. Dugas, B. Charleux, M. Lansalot and E. Bourgeat-Lami, *Macromolecules*, 2015, **48**, 545–556.
- 28 S. Rose, A. PrevotEAU, P. Elzière, D. Hourdet, A. Marcellan and L. Leibler, *Nature*, 2014, **505**, 382–385.
- 29 J. Song, L. Pu, J. Zhou, B. Duan and H. Duan, *ACS Nano*, 2013, **7**, 9947–9960.
- 30 Q. Yan and Y. Zhao, *Chem. Commun.*, 2014, **50**, 11631–11641.
- 31 A. Feng, C. Zhan, Q. Yan, B. Liu and J. Yuan, *Chem. Commun.*, 2014, **50**, 8958–8961.
- 32 Q. Yan, J. Wang, Y. Yin and J. Yuan, *Angew. Chem., Int. Ed.*, 2013, **52**, 5070–5073.
- 33 A. Darabi, P. G. Jessop and M. F. Cunningham, *Chem. Soc. Rev.*, 2016, **45**, 4391–4436.

